ORIGINAL PAPER

H$_2$S corrosion inhibition of an ultra high strength pipeline by carboxyethyl-imidazoline

E. F. Diaz · J. G. Gonzalez-Rodriguez ·
A. Martinez-Villafañe · C. Gaona-Tiburcio

Abstract The H$_2$S corrosion inhibition of ultra high strength steel with carboxyethyl-imidazoline has been evaluated with electrochemical techniques. Tested material included a water quenched Fe–C–Mn steel micro alloyed with Si, Nb, Cr, and Ti, equivalent to an API X-120 pipeline steel, whereas electrochemical techniques included polarization curves, linear polarization resistance, electrochemical impedance spectroscopy, and electrochemical noise measurements. Tested solutions included H$_2$S-containing 3% NaCl with and without 10 vol% of diesel and different inhibitor concentrations (0, 5, 10, 25, 50, and 100 ppm) at 50 °C. Different techniques have shown that the optimum carboxyethyl-imidazoline efficiency was obtained with 50 ppm, but the efficiency decreases as time elapsed. Corrosion rates obtained with diesel were lower than those obtained without diesel.

Keywords Sour corrosion · Corrosion inhibitor ·
X-120 steel · Electrochemical impedance

1 Introduction

Moving wet gas from offshore production facilities for onshore treatment, is often an economically attractive alternative, offshore drying, and allows more flexibility in field development. In several situations, offshore drying could not be considered as a feasible option, thus, making unrefined fluids transportation unavoidable. Fluid contains CO$_2$, H$_2$S, and acid in combination with highly corrosive water [1, 2]. Oilfield corrosion manifests itself in several forms, such as CO$_2$ corrosion (sweet corrosion), hydrogen sulfide (H$_2$S) corrosion (sour corrosion), and corrosion by dissolved oxygen in water injection, most prevalent forms of attack found in oil and gas production [3]. Due to its implications in different industries, corrosion of steel in H$_2$S-containing solutions is a well-known phenomenon that has been investigated for many years [4, 5]. The injection of corrosion inhibitor is a standard practice in oil and gas production systems to control internal corrosion of carbon steel structures. Nitrogen-based organic inhibitors, such as imidazolines or their salts have been successfully used in this application [6–8]. Corrosion inhibition by organic compounds is related to their adsorption properties that depend on the nature and the state of the metal surface, the type of corrosive environment and the chemical structure of the inhibitor [9–11].

Among the different electrochemical techniques that can be used to evaluate inhibitors, electrochemical impedance spectroscopy (EIS) is a powerful tool in addition to traditional techniques, such as polarization curves or linear polarization resistance (LPR) measurements. However, electrochemical noise (EN) measurements have also been successfully applied to the study of corrosion inhibitors performance [12–15]. These measurements are made without any external perturbation of the systems, and provide information about the actual system being studied with little possible artifacts.

Electrochemical noise (EN) technique involves the estimation of the electrochemical noise resistance R_n, which is calculated as the standard deviation of potential σ_v, divided by the standard deviation of current σ_i,

E. F. Diaz · A. Martinez-Villafañe · C. Gaona-Tiburcio
Centro de Inv. en Materiales Avanzados, Miguel de Cervantes 120, Chih, Mexico

J. G. Gonzalez-Rodriguez (✉)
U.A.E.M.-C.I.I.C.Ap, Av. Universidad 1001, 6225 Cuernavaca, MOR, Mexico
e-mail: ggonzalez@uaem.mx

$$R_n = \sigma_v / \sigma_i \qquad (1)$$

where R_n can be taken as the linear polarization resistance, R_p in the Stern–Geary equation:

$$I_{corr} = \left[\frac{(b_a + b_c)}{2.3 \, b_a b_c} \right] \cdot \frac{1}{R_p} \qquad (2)$$

thus, inversely proportional to the corrosion rate I_{corr}, but with the necessary condition that a trend removal applied over an average baseline, as previously established [16]. It has been demonstrated that the noise signal provides information about the dynamics that occur on the surface of the electrode and about the type of corrosion that is occurring, either uniform or localized. The aim of this study is to study the performance of a simple organic compound, carboxyethyl-imidazoline, as H_2S corrosion inhibitor of API X-120 pipeline steel using different electrochemical techniques, such as polarization curves, LPR, EIS, and EN measurements.

2 Experimental procedure

2.1 Testing material

Material tested was API X-120 pipeline with a chemical composition as given in Table 1, with an acicular ferrite + martensitic microstructure resulting from heating it at 867 °C 30 min and then water quenched.

2.2 Testing solution

The inhibitor used, in this study, was a commercial carboxyethyl-imidazoline with a general structure as shown in Fig. 1, which is composed of a five-member ring containing nitrogen elements, a C-14-saturated hydrophobic head group and a pendant, hydrophilic carboxyamido group attached to one of the nitrogen atoms. Inhibitor was dissolved in pure 2-propanol. The concentrations of the inhibitor were 0, 5, 10, 25, 50, and 100 ppm (molar) of inhibitor and the temperature kept at 50 °C. The testing solution was 3% NaCl, heated, de-aerated with nitrogen, H_2S was produced by reacting 3.53 mg l^{-1} sodium sulfide (Na_2S) with 1.7 mg l^{-1} acetic acid. Inhibitor was added 2 h after pre-corroding the specimen using a micro syringe. In order to simulate the oily phase present in real conditions inside a pipeline, some tests were performed by
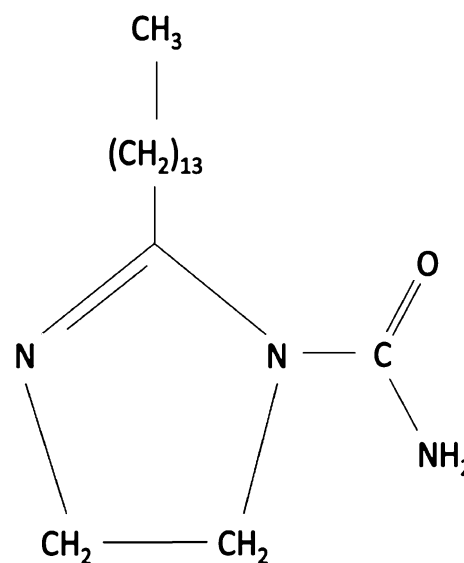

Fig. 1 General structure of carboxyethyl-imidazoline

adding 10 (vol%) of diesel to the H_2S-containing 3% NaCl solution.

2.3 Electrochemical measurements

The electrochemical techniques employed included potentiodynamic polarization curves, linear polarization resistance, LPR, EIS, and EN measurements, both in current and voltage. Polarization curves were recorded at a constant sweep rate of 1 mV s^{-1} from −300 to +300 mV interval with respect to the open circuit potential (E_{corr}). The measurements were obtained using a conventional three electrode glass cell with two graphite rods as auxiliary electrodes, and a saturated calomel electrode (SCE) as a reference electrode with a Lugging capillary bridge. Corrosion current density values, I_{corr}, were calculated using the Tafel extrapolation method by taking an extrapolation interval of ±250 mV with respect to the E_{corr} value once stable. The inhibitor efficiency η was calculated as follows:

$$\eta \, (\%) = \frac{(I_{corr} - I'_{corr})}{I_{corr}} \times 100, \qquad (3)$$

where I'_{corr} and I_{corr} are the corrosion current values with and without inhibitor, respectively. LPR measurements were carried out by polarizing the specimen ±10 mV with respect to E_{corr}, at a scanning rate of 1 mV s^{-1} every 20 min, for

**Table 1** Chemical composition of X-120 pipeline steel/wt%

C	Si	Mn	P	S	Cr	Mo	Ni	Al	Co	Cu	Nb	Ti	Fe
0.027	0.24	1.00	0.003	0.004	0.42	0.18	1.35	0.045	0.004	0.010	0.024	0.015	96.6

24 h. Electrochemical impedance spectroscopy tests were carried out at E_{corr} using a signal with an amplitude of 10 mV and a frequency interval of 0.1 Hz–30 kHz. An ACM potentiostat controlled by a desktop computer was used for the LPR tests and polarization curves, whereas for the EIS measurements a PC4 300 Gamry potentiostat was used. EN measurements in both current and potential were recorded using two identical working electrodes and a reference electrode (SCE). The EN measurements were made recording simultaneously the potential and current fluctuations at a sampling rate of 1 point per second. A fully automated zero resistance ammeter (ZRA) from ACM instruments was used in this case. Finally, the noise resistance R_n was then calculated as the ratio of the potential noise standard deviation σ_v over the current noise standard deviation σ_i, according to Eq. 1.

3 Results and discussion

Figure 2 shows the effect of carboxyethyl-imidazoline concentration on the polarization curves for API X-120 pipeline steel in H$_2$S-containing 3% NaCl solution at 50 °C. In all cases, the steel showed only an active behavior, anodic dissolution, without evidence of any passive layer. The shape of the curve practically remained the same with the addition of either 5 or 10 ppm of carboxyethyl-imidazoline. The E_{corr} value lies between −765 and −795 mV for these solutions whereas the corrosion current density value, I_{corr}, was around 10^{-4} mA cm^{-2}. The corrosion rate obtained with 5 ppm of carboxyethyl-imidazoline was slightly higher than that of the uninhibited solution, 3×10^{-4} mA cm^{-2}. With 25 ppm of inhibitor, the I_{corr} value was reduced to 6×10^{-6} mA cm^{-2} whereas with 50 ppm of carboxyethyl-imidazoline this value reached its lowest value, 4×10^{-6} mA cm^{-2}, and the noblest E_{corr} value was obtained. When the inhibitor concentration increased further to 100 ppm, the I_{corr} value was similar to that obtained for the blank, uninhibited solution, 9×10^{-5} mA cm^{-2}, and the E_{corr} value was −795 mV. It seems that the optimum inhibitor concentration lies between 25 and 50 ppm. Table 2 summarizes the electrochemical values obtained from polarization curves.

The effect of carboxyethyl-imidazoline concentration on the change in the R_p values with time for API X-120 pipeline steel in the H$_2$S-containing 3% NaCl solution is shown in Fig. 3. The highest R_p value, and, thus, the lowest I_{corr} was obtained with the addition of either 25 or 50 ppm of carboxyethyl-imidazoline. However, the R_p value obtained with 25 ppm of inhibitor decreases very rapidly whereas that obtained with 50 ppm remained the highest. On the other hand, the lowest R_p was obtained for the blank solution and with the addition of either 5 or 100 ppm of
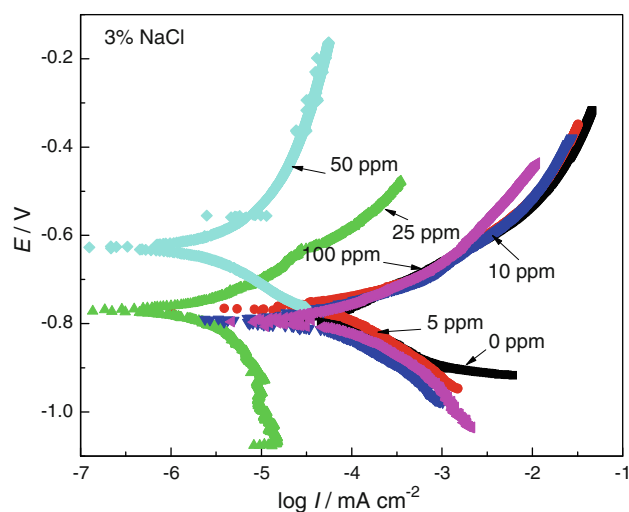
Fig. 2 Effect of carboxyethyl-imidazoline concentration on the polarization curves for X-120 pipeline steel in H$_2$S-containing 3% NaCl solution

**Table 2** Electrochemical parameters obtained from polarization curves in H$_2$S-containing 3% NaCl solution

Inhibitor concentration (ppm)	E_{corr} (mV)	I_{corr} (mA cm^{-2})	η (%)
0	−792	2×10^{-4}	–
5	−765	3×10^{-4}	−50
10	−795	1×10^{-4}	50
25	−775	6×10^{-6}	97
50	−630	4×10^{-6}	98
100	−795	9×10^{-5}	55

Table 3 Electrochemical parameters obtained from polarization curves in H$_2$S-containing 3% NaCl + diesel solution

| Inhibitor concentration (ppm)	E_{corr} (mV)	I_{corr} (mA cm^{-2})
0	−785	1×10^{-4}
50	−685	8×10^{-6}

carboxyethyl-imidazoline. In solutions containing H$_2$S, the corrosion of steel is generally accompanied by the formation of iron sulfide film [16, 17]. The fact that R_p decreased with time, suggests the non-protective nature of the corrosion products film. The film, a non-adherent layer which can be easily removed from the steel surface, did not passivate the steel surface under the environmental conditions used here. The protectiveness of the inhibitor film should depend on other factors, upon the adherence and stability of the inhibitor on this iron sulfide film. As soon as the inhibitor was added, the R_p value increased, and thus, the corrosion rate decreased. R_p reached its highest value with 50 ppm of inhibitor. For lower or higher inhibitor concentrations, the R_p value was lower than that obtained
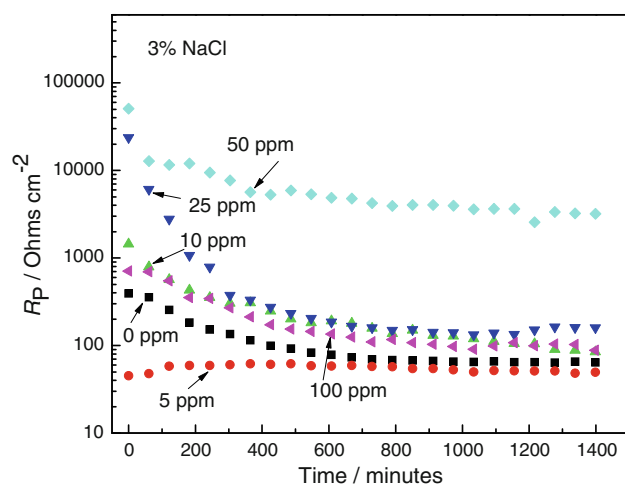
Fig. 3 Effect of carboxyethyl-imidazoline concentration on the change in the R_p values with time for X-120 pipeline steel in H$_2$S-containing 3% NaCl solution

with 50 ppm. However, R_p decreased with time, showing an increase in the corrosion rate. Organic inhibitors normally form a protective layer on the surface of the metal. However, the decrease in the R_p value shows that the inhibitor was unstable and detached from the metal surface. The metal remains unprotected and exhibits a higher corrosion rate, evident with the addition of 100 ppm of carboxyethyl-imidazoline.

Nyquist data for API X-120 steel in uninhibited H$_2$S-containing 3% NaCl solution is shown in Fig. 4. The impedance spectra show a single capacitive-like, depressed semicircle, indicating a process under charge transfer control. In such a process, the semicircle diameter, the charge transfer resistance R_{ct} is equivalent to the linear polarization resistance value R_p. It can be seen that the semicircle diameter increased with time up to 4 h, which
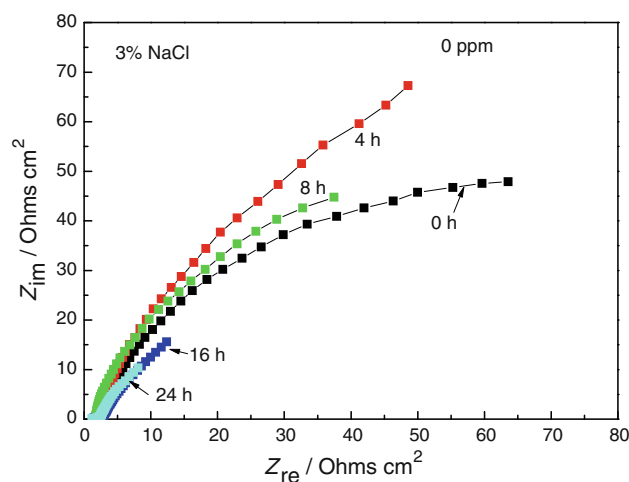
Fig. 4 Nyquist diagram for X-120 pipeline steel in uninhibited H$_2$S-containing 3% NaCl solution

indicates that the corrosion rate decreased as time elapsed. The fact that the semicircle diameter increased first over time and after a while it decreased, suggests the non-protective nature of the corrosion products film. This film is a non-adherent layer which can be easily removed from the steel surface and does not passivate the steel surface under the environmental conditions used here. However, after 4 h approximately, the semicircle diameter decreased as time elapsed, indicating an increase in the corrosion rate. In H$_2$S-containing solutions, the corrosion process of iron and steel is generally accompanied by iron sulfide film formation [16, 17]. Thus, the increase in the impedance is due to the growth of iron sulfide film. The decrease in the semicircle diameter indicates that film growth continues until a critical thickness, after which the film cracks and becomes detached from the metal surface. This suggests that the non-protective nature of the corrosion product. This is in agreement with the results reported by Vedage et al. [18] for 4130 steel in H$_2$S solution at 95 °C that the corrosion process for short times was film-diffusion limited, whereas for longer times, a steady state was reached, where the film growth was balanced by its dissolution into the aqueous phase, leading to a limited film thickness. Huang et al. [19] working with carbon steel in H$_2$S solution at 25 °C reported, at an early stage, a large semicircle with its impedance increasing with time. At a later stage, the precipitation of sulfide film revealed the presence of a second capacitive semicircle at lower frequency values. In a similar way, Arzola et al. [20], when working with API X-70 pipeline steel in a H$_2$S-containing 3 wt% NaCl solution at 25 °C, reported that the Nyquist diagrams showed that the presence of one loop at high frequencies and an uncompleted loop at lower frequencies. However, under dynamic conditions, with 1,000 rpm in a rotating disc electrode, only one capacitive-like semicircle. Under static conditions, the increase in the semicircle diameter value with time during the first hour has been reported by Arzola et al. [20] to be due to the growth of an iron sulfide film, whereas a decrease to the dissolution of this film.

When 50 ppm of carboxyethyl-imidazoline were added (Fig. 5), the data described a straight line at high frequencies, indicating that the corrosion process was now under diffusion control, through an inhibitor-formed film, whereas at low frequencies a depressed, capacitive-like semicircle was observed, which correspond to a charge-transfer-controlled corrosion process. According to Ramachandran [10], the film formed by the presence of long hydrocarbon chains in the structure of the imidazoline acts as a protective barrier against aggressive ions from the bulk solution. Thus, the corrosion process, when 50 ppm of carboxyethyl-imidazoline was added, was under diffusion and charge transfer mixed mechanism. Unlike the uninhibited solution, the total impedance in the presence of the
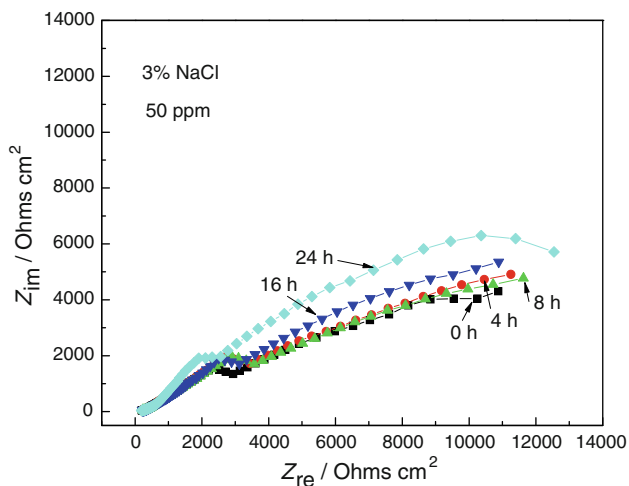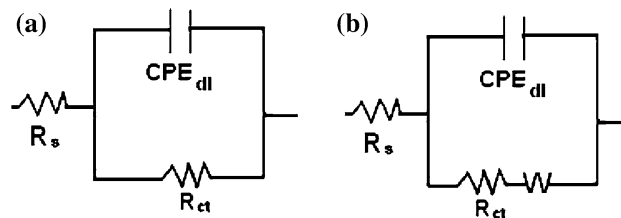
Fig. 5 Nyquist diagram for X-120 pipeline steel in H$_2$S-containing 3% NaCl solution with 50 ppm of carboxyethyl-imidazoline

Fig. 6 Electric circuits used to simulate the EIS data for X-pipeline steel in the H$_2$S-containing 3% NaCl containing **a** 0 and **b** 50 ppm of carboxyethyl-imidazoline

Table 4 Calculated parameters used to simulate the EIS data for X-120 pipeline in uninhibited H$_2$S-containing 3% NaCl solution

Time (h)	R_s (Ohms cm^2)	Y_{dl} (Ohms^{-1} s^n)	n_{dl}	R_{ct} (Ohms cm^2)
0	6	2.5×10^{-2}	0.52	96
4	6.5	9.1×10^{-2}	0.75	107
8	6.5	4.1×10^{-2}	0.83	84
16	6.6	3.7×10^{-2}	0.78	69
24	7.9	3.0×10^{-2}	0.79	51

inhibitor increased with time, showing the protective nature of the inhibitor film formed. It can also be seen that the semicircle diameter obtained with 50 ppm of inhibitor was almost one order of magnitude bigger than that obtained for the blank solution, in agreement with polarization curves (Fig. 2) and the LPR measurements (Fig. 3).

The EIS data were simulated using equivalent electric circuits as shown in Fig. 6, where R_s represents the solution or electrolyte resistance, C_{dl} the double layer capacitance, R_{ct} the charge transfer resistance, W represents the Warburg impedance, given by:

$$W_0 = R_w \coth(j\omega s)^\alpha / (j\omega s)^\alpha, \qquad (4)$$

where $s = \lambda^2/D$, with λ as the thickness of the diffusion layer, D is the diffusion coefficient of the species involved, and R_w the resistance of the diffusion layer. When a non-ideal frequency response is present, it is commonly accepted to use distributed circuit elements in an equivalent circuit. The most widely used is constant phase element (CPE), which has a non-integer power dependence on the frequency. The impedance of a CPE is described by the expression:

$$Z_{CPE} = Y^{-1}(j\omega)^{-n} \qquad (5)$$

where Y is a proportionality factor, j is $\sqrt{-1}$, ω is $2\pi f$ and n a phase shift. Often, a CPE is used in the model instead of a capacitor to compensate for non-homogeneity in the system. Parameters used to simulated EIS data are shown in Tables 4 and 5 for uninhibited and inhibited solutions, respectively.

The combined effect of potential standard deviation σ_v and current standard deviation σ_i resulted in the noise resistance value R_n (Eq. 1) which is inversely proportional to the corrosion rate I_{corr} for the different inhibitor concentrations, as shown in Fig. 7. This behavior is similar to that observed in Fig. 3 by R_p; initially R_n was high and corresponds to a low corrosion rate; low R_n values observed toward the end of testing correspond to an increase in the corrosion rate. This fact shows that the inhibitor remains for a short time on the metal surface; the highest R_n value, the lowest corrosion rate, was obtained with the addition of

Table 5 Calculated parameters used to simulate the EIS data for X-120 pipeline in H$_2$S-containing 3% NaCl + 50 ppm carboxyethyl-imidazoline solution

Time (h)	R_s (Ohms cm^{-2})	CPE$_{dl}$		W_0			R_{ct} (Ohms cm^{-2})
		Y_0 (Ohms^{-1} s^n)	n_{dl}	R_w (Ohms cm^{-2})	s	α	
0	236	4.0×10^{-3}	0.39	8,622	31	0.39	9,848
4	245	3.7×10^{-4}	0.43	9,983	21	0.55	11,520
8	303	3.1×10^{-4}	0.44	11,784	10	0.72	16,729
16	250	3.8×10^{-4}	0.39	13,003	3.5	0.84	22,366
24	221	1.2×10^{-4}	0.55	7,089	6.4	0.59	14,110
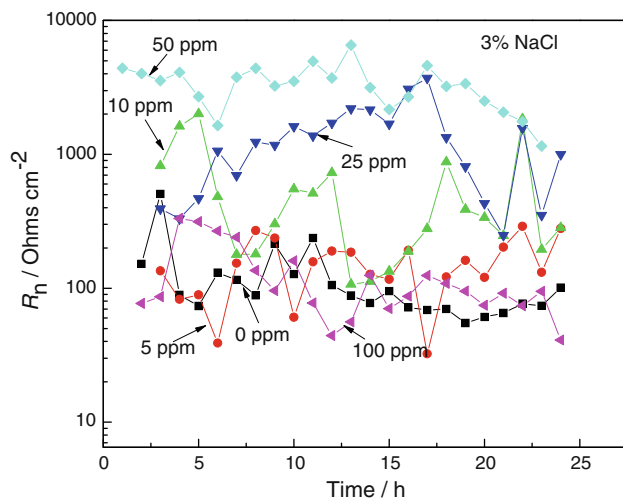
Fig. 7 Effect of carboxyethyl-imidazoline concentration on the change in the R_n values with time for X-120 pipeline steel in H$_2$S-containing 3% NaCl solution

Fig. 8 Polarization curves for X-120 pipeline steel in H$_2$S-containing 3% NaCl + diesel solution with **a** 0 and **b** 50 ppm of carboxyethyl-imidazoline

50 ppm of carboxyethyl-imidazoline followed by the addition of 25 ppm of inhibitor, whereas the lowest R_n value, the highest corrosion rate, was obtained for the blank solution or with the addition of either 5 or 100 ppm of carboxyethyl-imidazoline. Thus, corrosion rates estimated by both polarization curves and LPR measurements were similar to those obtained by EN measurements, indicating that the optimum carboxyethyl-imidazoline concentration in the H$_2$S-containing 3% NaCl solution at 50 °C was 50 ppm. An optimum corrosion inhibitor concentration was also found by Ma et al. [21], who found that H$_2$S can either accelerate or inhibit corrosion of iron under different experimental conditions, such as H$_2$S concentration and solution pH. The inhibition effect of H$_2$S was attributed to the formation of FeS protective film for H$_2$S concentrations below 0.04 mmol cm^{-3}. Similarly, Abelev et al. [22] examined the effect of H$_2$S at ppm level concentrations on iron corrosion in 3 wt% NaCl solutions saturated with CO$_2$ in the temperature range of 25–85 °C using electrochemical and surface science techniques. Small H$_2$S concentrations (5 ppm) had an inhibiting effect on corrosion in the presence of CO$_2$ at temperatures from 25 to 55 °C. At 85 °C, however, 50 ppm H$_2$S was needed to provide significant corrosion inhibition. At higher H$_2$S concentrations, the corrosion rate increased rapidly, while still remaining below the rate for the H$_2$S-free solution. Thus, these research works reported a peaking effect of inhibitor concentration ascribed to the formation of an inhibitive film which then breaks down at higher concentrations.

In order to simulate the effect of the oily phase present inside the pipeline, 10 vol% of diesel was added to the 3% NaCl solution. Figure 8 shows polarization curves for API X-120 pipeline steel with and without inhibitor, 50 ppm of
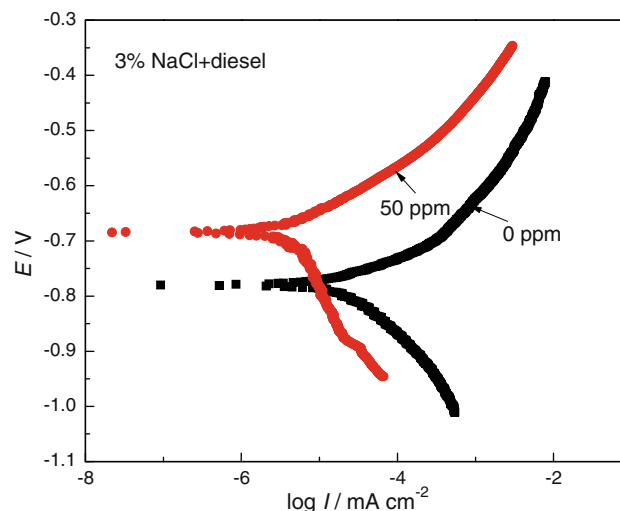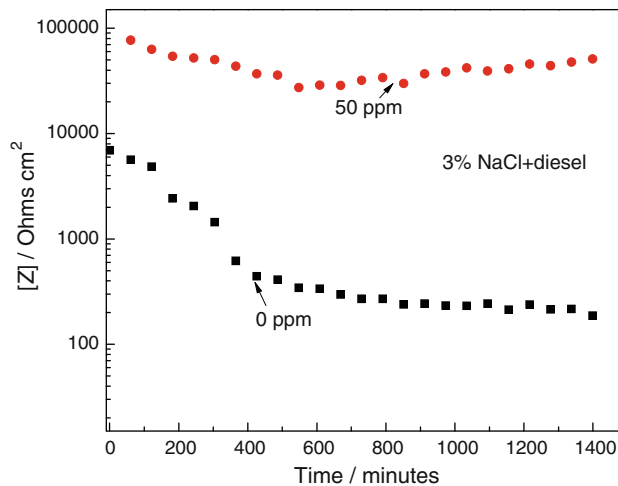
carboxyethyl-imidazoline, in the H$_2$S-containing 3% NaCl + diesel solution. In both cases, the steel displayed an active behavior, without any evidence of a passive layer. With the addition of the inhibitor, the E_{corr} value was made nobler and the I_{corr} value was decreased by nearly two orders of magnitude as compared to the uninhibited solution. Table 3 summarizes the electrochemical parameters for the diesel-containing solution.
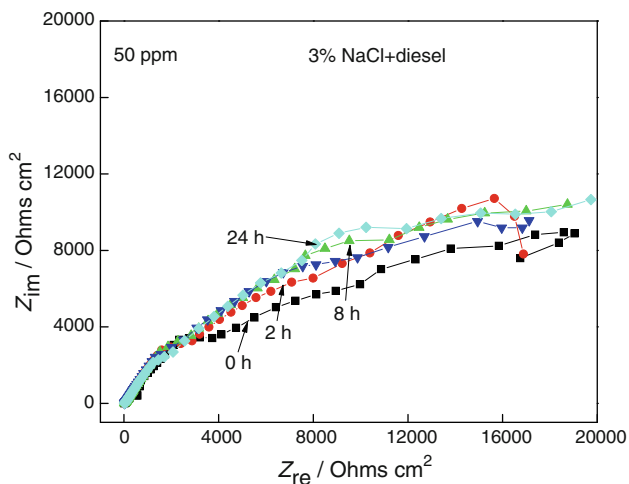
The Nyquist diagram for API X-120 pipeline steel in the uninhibited H$_2$S-containing 3% NaCl + diesel solution is shown in Fig. 9. The data describe 2, capacitive-like, depressed semicircles, with the centers in the real axis. The semicircle at high frequencies has been related to the charge transfer from the metal to the solution, whereas the second semicircle at low frequencies is related to the formation of a film formed by the diesel. The total impedance value [Z] decreases with time, indicating that the corrosion rate decreases in the presence of the oily phase. With 50 ppm of carboxyethyl-imidazoline added to the 3% NaCl + diesel solution (Fig. 10), the EIS data describes three semicircles in the Nyquist diagram, with the total impedance [Z] remaining more or less constant with time. The high frequency semicircle corresponds to the charge transfer from the metal to the solution, the second semicircle at intermediate frequencies corresponds to the formation of a film formed by the oily phase, and the third, low frequency semicircle corresponds to the formation of a film formed by the inhibitor. Figure 11 presents the change in the total impedance [Z] for both uninhibited and inhibited H$_2$S-containing 3% NaCl + diesel solutions. Compared with the R_p value for the uninhibited solution (Fig. 3), the data for the uninhibited solution in the presence of diesel was slightly higher, decreasing the corrosion rate. Second, the data for the solution with 50 ppm of
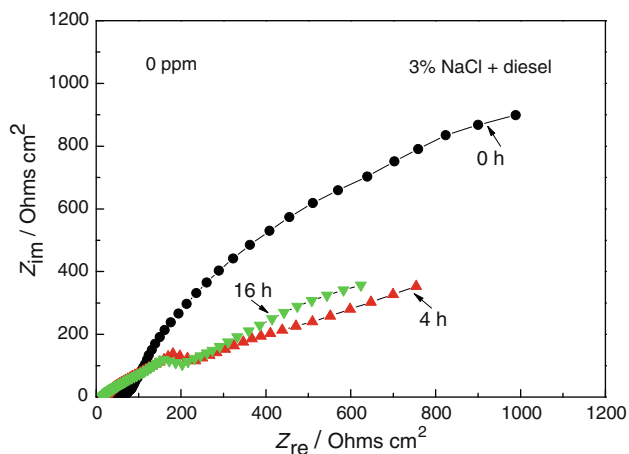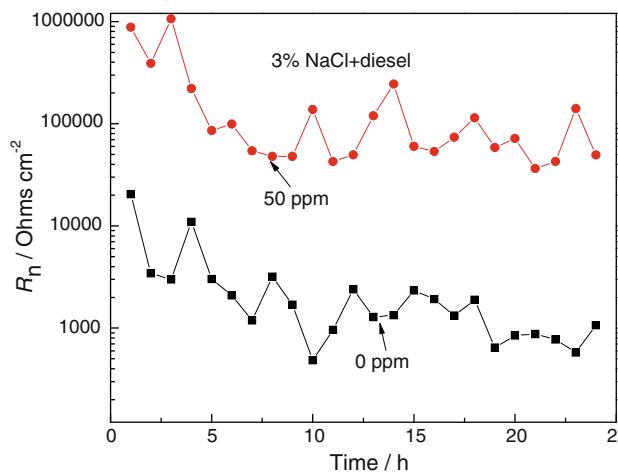
Fig. 9 Nyquist diagram for X-120 pipeline steel in uninhibited H₂S-containing 3% NaCl + diesel solution

Fig. 11 Change on the impedance modulus, [Z] for X-120 pipeline steel in H₂S-containing 3% NaCl + diesel solution with 0 and 50 ppm of carboxyethyl-imidazoline

Fig. 10 Nyquist diagram for X-120 pipeline steel in H₂S-containing 3% NaCl + diesel solution with 50 ppm of carboxyethyl-imidazoline

Fig. 12 Change on the noise resistance value with time R_n for X-120 pipeline steel in H₂S-containing 3% NaCl + diesel solution with 0 and 50 ppm of carboxyethyl-imidazoline

carboxyethyl-imidazoline in the presence of diesel were similar in magnitude, but remained more constant with time than in the absence of diesel. This is expected since the inhibitor used was oil soluble and the inhibitor can be transported easier to the surface. Thus, it seems that the presence of diesel has an effect of co-adsorption of the inhibitor on the substrate, which improves its performance.

The combined effect of potential standard deviation σ_v and current standard deviation σ_i gives the noise resistance value R_n for the H₂S-containing 3% NaCl + diesel solution (Fig. 12), which shows an identical behavior to that exhibited by total impedance (Fig. 11). The R_n data for the inhibited solution was almost two orders of magnitude higher than that for the uninhibited solution. The behavior of R_p and R_n in the presence of the oily phase is similar to that in the absence of diesel: high values at the beginning

of the test, and low values toward the end of the test, indicating a slightly longer residence time of the inhibitor in the presence of the oily phase.

Quiroga et al. [23] carried out corrosion tests with an AISI 1010 carbon steel using diesel-in-water emulsions, with 0.2 wt% NaCl as base solution. The oily phase (diesel) facilitates the cathodic partial reduction of oxygen reaction due to the enhanced solubility of oxygen compared with water, while inhibiting the dissolution of the metal. In this study, corrosion rates obtained in the presence of diesel were slightly lower than those obtained without diesel. This can be explained in terms of the coverage given by the oily phase on the metal surface. The surface coverage of a solution in the presence of an inhibitor θ is given by:

$$\theta = \eta/100 \qquad (6)$$

where η is the inhibitor efficiency as given by Eq. 3. As shown in Table 2, the highest coverage given by the carboxyethyl-imidazoline was obtained with 50 ppm, which indicates that the whole surface was covered by the inhibitor. According to Fig. 3, the corrosion rate of the metal increased in all cases, regardless the presence of inhibitor, which indicates that the surface covered by the inhibitor decreased with time, leaving active sites where corrosion takes place. The fact that the R_n values in the presence of diesel were higher than the corresponding R_p values, might indicate that localized activity such as pitting type of corrosion could occur on the active sites left uncovered by the film formed by diesel.

4 Conclusions

The effect of carboxyethyl-imidazoline concentration on the H_2S corrosion inhibition of API X-120 pipeline steel in 3% NaCl solution at 50 °C has been studied using different electrochemical techniques. In the absence of diesel, the best corrosion inhibition was reached with the addition of 50 ppm of carboxyethyl-imidazoline with an efficiency of 98%. However, this efficiency decreased with time, indicating a short residence time of the inhibitor. In the presence of diesel, the corrosion rate was lower to that obtained without diesel.

References

1. Tresseder RS (1981) Oil industry experience with hydrogen embrittlement and stress corrosion cracking. In: Tuttle RN, Kane RD (eds) H_2S corrosion in oil and gas production: a compilation of classic papers. NACE, Houston, TX, p 147
2. Kapusta SD, Pots BFM (1998) The materials and corrosion view of wet gas transportation. In: Jackman PS, Smith LM (eds) Advances in corrosion control and materials in oil and gas production. European Federation of Corrosion Publications 26. Woodhead Publishing, Abington, p 5
3. Kermani MB, Morshed A (2003) Corrosion 59:659
4. Smith SN (1993) A proposed mechanism for corrosion in slightly sour oil and gas production. Proceedings of the 12th International Corrosion Congress held in September 19–23 Houston, TX, NACE International
5. Foroulis ZA (1993) Corros Prev Control 40:84
6. Jovancicevic V, Ramachandran S, Prince P (1999) Corrosion 55:449
7. Ramachandran S, Jovancicevic V (1999) Corrosion 55:259
8. Xueyuan Z (2001) Corros Sci 43:1417
9. Bentiss F, Lagrenee M, Traisnel M, Hornez JC (1999) Corros Sci 41:789
10. Ramachandran S, Tsai M, Blanco M, Chen H, Tang WA (1996) Langmuir 12:6419
11. Wang D, Li S, Ying M, Wang M, Xiao Z, Chen Z (1999) Corros Sci 41:1911
12. Popova A, Raicheva S, Sokolova E, Christov M (1996) Langmuir 12:2083
13. Nykos L, Pajlossy T (1985) Electrochim Acta 30:1533
14. Garcia-Ochoa E, Genesca (2004) J Surf Coat Technol 184:322
15. Samiento-Bustos E, González Rodriguez JG, Uruchurtu J, Dominguez-Patiño G, Salinas-Bravo VM (2008) Corros Sci 50:2296
16. Tewart PH, Campbell AB (1979) Can J Chem 57:188
17. Meyer FH, Riggs OL, McGlasson RL, Sudbury JD (1958) Corrosion 14:69
18. Vedage H, Ramanarayanan TA, Mumford JD, Smith SN (1993) Corrosion 49:114
19. Wang HH, Tsay WT, Lee JT (1996) Electrochim Acta 41:1191
20. Arzola S, Mendoza-Florez J, Duran-Romero R, Genesca J (2006) Corrosion 62:433
21. Ma HY, Cheng XL, Li GQ, Chen SH, Quan ZL, Zhao SY, Niu L (2000) Corros Sci 42:1669
22. Abelev E, Sellberg J, Ramanarayanan TA, Bernasek SL (2009) J Mater Sci 44:6167
23. Quiroga-Becerra H, Retamoso C, Macdonald Digby D (2000) Corros Sci 42:561